Journal of Geology & Geophysics

Epuh and Joshua, J Geol Geophys 2017, 6:2
DOI: 10.4172/2381-8719.1000285

Research Article | Open Access

Basement Depth and Sedimentary Velocity Structure in Gongola Basin

Epuh EE[1*] **and Joshua EO**[2]

[1]*Department of Surveying and Geoinformatics, University of Lagos, Nigeria*

[2]*Physics Department, University of Ibadan, Nigeria*

***Corresponding author:** Epuh EE, Department of Surveying and Geoinformatics, University of Lagos, Nigeria, Tel: +23412802439; E-mail: eeepuh@yahoo.com

Received date: January 30, 2017; **Accepted date:** March 15, 2017; **Published date:** March 23, 2017

Abstract

Basement depth in the Gongola basin is found to be much deeper than previously supposed. Gravity modelling of the upper Benue Trough, Nigeria revealed thick sedimentation with maximum values within the range 5.2 km-7.0 km. This is in contrast to the average value of 5.0 km suggested by earlier studies. Gravity modelling across the basin was carried out to determine the basement depth using the second vertical derivative as input anomaly profile. The seismic modelling process in this research involves the determination of the distribution of seismic velocity using the: depth-normalized velocity iteration technique, check shot and sonic log curves. The integrated depth algorithm (IDA) iterative process was adopted in the determination of the interval and depth normalized interval velocities to adequately address the depth conversion for the determination of the lithology of the basin. The localized nature of the interpreted velocity data were extrapolated away from and interpolated between acquisition location using the areal coverage provided by gravity and seismic data. The interpretation involves the integration of the seismic reflection profiles, well logs and potential field data to establish a model of the sedimentary thicknesses and seismic velocities throughout the basin. The Basement depth on the north east of the basin is 7.0 km, southeast is 5.2 km whilst the northwest and southwest ranges between 0.5 km and 1.0 km respectively. The basement depths obtained from the gravity model was compared with that obtained from reflection seismic observation from the study area and the relative error percent were 1.37% and 0.46% respectively. The Precambrian basement depth normalized interval velocities ranges between 6.2 km/s and 6.4 km/s respectively. The qualitative interpretation of the second vertical derivative shows that the rift architecture/geometry is controlled by high angle faults and extended graben structures that form the major depocenters that are predominant in the upper Benue rift system. The grabens, half grabens, faults and deep sedimentation interpreted from the seismic reflection data are hydrocarbon related structural features. Consequently, the potentially hydrocarbon (gas) rich Yolde/Bima (Cenomanian-Albian) stratigraphic formations at depth between 2.1 km and 2.7 km and the depth normalized interval velocity varies from 2.9 km/s to 3.3 km/s and it occurs within the southeast zone of the basin.

Keywords: Basement depth; Second vertical derivative; Interval velocity; Depth normalized interval velocity; Sedimentary basin

Introduction

The main purpose of a gravity survey over a sedimentary basin is to delineate the configuration of the basin. Sedimentary basins are generally associated with low gravity values due to the low density sediments in them. In general, the density of sedimentary rocks in a basin increases with depth [1]. In some basins, this variation depends on several factors. In such situations, the gravity modelling can be carried out assuming variable density which plays an important role in accurate determination of basement depths under the sedimentary cover.

While sedimentary rocks often have density values below 2.40 g/cm^3 mafic igneous and plutonic rocks have density values above 3.00 g/cm^3. Martinec showed theoretically that small lateral density variation of topographic masses may introduce errors on the depth determination [2]. Mapping of depth-to-basement results shows image of basement topography that provides information about the position, shape and depth of overlying basins and the thickness of the overlying sediments. By understanding the shape and structural controls of a basin early in an exploration program, exploration concepts at the petroleum system and play level can be evaluated better and more efficiently.

The application of depth conversion using only the check shot curve technique sometimes fail in areas of complex structures, tectonic inversion or lateral velocity change where insufficient well controls exist to adequately define the velocity variations in different lithologic units [3]. In the Gongola Basin, the well information is sparse and the analysis of seismic reflection data had relied heavily on structural mode. This reliance on structural mode is necessary in view of the fact that seismic images of fold and thrust structures within the area are distorted and of uneven quality. Part of the strata geometry may be clearly shown while others show either a lack or a confusing surplus of reflection signals.

Migrated results of uniform quality are difficult to obtain especially where seismic imaging is poor because of the complex structural geometry of the basin. Apart from the strong basement reflections over some areas, there are no real characteristics seismic markers and this makes correlation very tenuous. This article also examines the application of depth normalized interval velocity computed using the integrated depth algorithm (IDA) iterative process to adequately address the depth conversion for the determination of the lithology of the basin.

Citation: Epuh EE, Joshua EO (2017) Basement Depth and Sedimentary Velocity Structure in Gongola Basin. J Geol Geophys 6: 285. doi: 10.4172/2381-8719.1000285

Geological Background

The Benue Trough is located at a major re-entrant in the West African continental margin. It is bordered to the south-west by the Cenezoic Niger Delta and extends transversely northwards to the Chad basin. The margins of the Benue Trough are collinear both the Charcot and chain fracture zones of the equatorial Atlantic. The evolution of the Benue Trough is closely linked with the opening of the South Atlantic. Details on the sequence of events that led to its formation alongside other sedimentary basins in Nigeria are contained in the various literatures [4-8]. It is a rift basin with plate dilation leading to the opening of the Gulf of Guinea [9,10]. Benkhelil also suggested that the evolution trough could also be as a result of tension resulting in a rift or wrench related fault basin [9].

Mesozoic to Cenezoic magmatism has accompanied the evolution of the tectonic rift as it is scattered all over and throughout in the trough [11,12]. A magmatic old rift was also suggested for the Gongola basin by Shemang et al. [13] while Abubakar et al. suggested the evolution as a combination of mantle upwelling or rise of a mantle plume which resulted in crustal stretching and thinning and the emplacement of basic igneous material within the basement and sediment which resulted in rifting [12].

The Benue Trough trends NE-SW and the northernmost end (upper Benue Trough) bi-furcates into two arms-the Gongola and the Yola arms (sub basins). The Gongola basin of the upper Benue Trough is a North-South trending arm of the 1000 km long Benue Trough.

These sub basins contain thick sediment accumulations (mainly Cretaceous) in excess of 5 km deposited under varying environments. The sediments have been subjected to main tectonic phases which account for the observed folding, faulting and fracturing of the rocks. Reviews of the geology and stratigraphic successions in the Benue Trough with details on each formation, bed thickness, lateral extensions and stratigraphic locations are found in Carter et al. [14], Petters [15], Petters and Ekweozor [16], Obaje [17], Obaje et al. [18].

Details on the evolution and stratigraphic framework of the Chad basin are given in Avbovbo et al. [19] and Olugbemiro et al. [20]. Depth determination by Ofoegbu and Onuoha [21] gave ranges in depth to basement between 1200 m-2500 m and they concluded that this part of the Benue Trough may not hold promise in terms of hydrocarbon accumulations. Review of other studies on the Benue Trough using potential field (magnetics and gravity) methods estimated the thickness of the Cretaceous sediments to be in the neighbourhood of 5000 m [22].

These include two dimensional models of Cratchley and Jones [5], Adighije [23], Ajayi and Ajakaiye [24] and the three dimensional (3-D) gravimetric study by Okereke et al. [25] gave the thickness of the Cretaceous sediment to be within a maximum range of 5000 m.

This study presents data that show deeper sedimentation in the trough which explain the basement structuring in the trough. Therefore, one of the objectives of this study is to demonstrate a deep sedimentation in upper Benue Rift and to reveal internal basin geometry.

Additional objective is to unravel subtle structural features and their trend within the upper Benue Rift and their control on sedimentation and subsequent rock deformation. The most important subtle structural features are minor vertical/high angle basement faults and zones of fracturing [22].

These are difficult to detect with seismic data because of the limitations of the seismic method in imaging near vertical structures such as faults and in penetrating high acoustic impedance layers such as sill [26] but can be mapped confidently with gravity second vertical derivative method.

This is because gravity method responds best to vertical interfaces generating lateral gravitational changes across a bounding fault and separating basement from sedimentary features. Where the sedimentary section is considerably thick, the amplitudes of the basement subtle features are attenuated and may be overlooked (Figure 1).

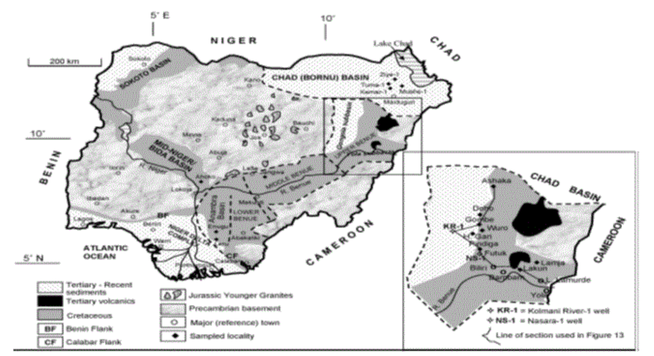

Figure 1: Sketch geological map of Nigeria showing the inland basins and sample localities. (Inset: upper Benue trough magnified [18]).

Mapping these subtle features in the gravity second vertical derivative data is significant in understanding basin framework of the upper Benue rift and their control on subsequent deformation. Thus, we used the derivative the map to achieve our objectives and inferring their tectonic and hydrocarbon implications.

In sedimentary basins, basement faults are important structurally because they can influence and hence determine the overall basin architecture, tectonic history and control on mineralization sites, oil and gas traps and groundwater flow pattern [27].

The Benue Trough is filled with sediments of Cretaceous (Albian-Maastrichtian) age. The sediments are made up of sandstones, shales and limestone and underlain by Precambrian basement (granites and gneisses). The earlier (Albian-Santonian) sediments in the trough are mainly marine in character and their deposition was terminated by the episode of deformation in the Santonian.

Following this deformation the marine sediments were eroded and deltaic sediments spread throughout the trough. Continental facies sedimentation persisted until the end of the Cretaceous, apart from short-lived but extensive marine incursion in the Maastrichian [22,28,29].

Petters [30] documented the main stages of tectonic evolution of the Benue Trough in stratigraphic succession. These include three depositional sequences; an Albian-Cenomanian pyroclastic, paralic shallow marine and fluviatile sequence corresponding to the graben and transitional tectonic stages.

The subsequent stages include a Turonian–Conniacian paralic, marine and fluviatile sequence that gave rise to downwarping and resulting widespread marine transgression [22]. The Santonian compressional deformation episode that displaced the depositional axis westward was followed by a Campanian-Maastrichian paralic, marine and fluviatile off lap sequence.

Model Formulation

Second Vertical Derivative (SVD) model formulation

Second vertical derivative (which gives a measure of the difference of the gravity values at a point relative to its values at neighbouring point) will be greater over the localized feature than over the more smoothly varying regional trend.

Second vertical derivatives are regarded as high pass filters that enhance anomalies caused by small features while suppressing longer wavelength regional trends [31]. In this study, the density of the sedimentary structure is considered to varying exponentially with depth [1]

$$\Delta p = \rho_0 e^{-\zeta z} \qquad (1)$$

where, r_o is the density contrast observed at the ground surface and z is a constant expressed in Km^{-1}. These values can be estimated by fitting equation (1) to the known density contrast-depth data of sedimentary rocks.

Based on the principle of density increase with depth, according to Bullard and Cooper [32], the second vertical derivative of a gravity field measured at discrete points on the earth's surface is given as:

$$\Delta g_{SVD}(x,y) = M_j(\gamma)\Delta g_0(x,y) \qquad (2)$$

$M_j(\gamma) =$ Weighting coefficient

$\Delta g_0(x,y) =$ Bouguer gravity anomaly at the surface

$$M_j(\gamma) = \frac{s^2}{a^2} e^{\frac{w_j}{2\pi}} \qquad (3)$$

$a =$ grid spacing, $s =$ shot point spacing

$$w_j = ua \qquad (4)$$

$u =$ wave number

The above expression is the second vertical derivative function to a depth of one grid unit a below the origin of coordinates.

Since the signal is projected to the depth of basement, the energy spectrum is reduced through absorption as it passes through the various sedimentary layers. Thus for low frequencies, the absorption is proportional to the square of the frequencies per wave numbers [33].

$$\varepsilon = \gamma u^2 \qquad (5)$$

$\varepsilon = absorption$ coefficient

Introducing equation 4 into equation 5, the expression for $w_j=ua$ is redefined as:

$$w_j = ua - \varepsilon = ua - \gamma u^2 \qquad (6)$$

Potential field anomalies are band-limited; that is, the Fourier transforms decay with increasing wave numbers. For efficient treatment of the anomalies, the Nyquist wave number was adopted. The Epuh et al [34] model gives the second vertical derivative as:

$$M_j(\gamma) = \frac{s^2}{a^2} e^{\frac{1}{2\pi}(ua - \gamma u^2)} \qquad (7)$$

$$\Delta g_{SVD}(x,y) = \frac{s^2}{a^2} e^{\frac{1}{2\pi}(ua - \gamma u^2)} \Delta g_0(x,y) \qquad (8)$$

$$u = \sqrt{u_x^2 + u_y^2} \qquad (9)$$

$$u_x = \frac{\pi}{x_m}, u_y = \frac{\pi}{y_m}$$

where $\Delta g_{SVD}(x,y) =$ the gravity anomaly projected to the basement depth d $\Delta g_0(x,y) =$ the observed gravity anomaly value at the surface.

$M_j(\gamma) =$ the weighting coefficent, a= grid spacing,

$\gamma =$ attenuation, s=distance between stations

x_m and $y_m =$ measured distances between points at which Δg takes the value $\frac{1}{2}\Delta g_{max}$ in these two directions.

Basement depth model formulation using Second Vertical Derivative as input anomaly profile

From equation 9 [34], ux and uy are wave numbers whose wavelengths correspond to $\frac{\pi}{x_m}$ and $\frac{\pi}{y_m}$ respectively. If we assume that the greater part of the basement corresponds to the ratio of the wave numbers. According to Epuh et al. [34] $\frac{u_x}{u_y} = \frac{y_m}{x_m} = \tau \qquad (10)$

Then the basement depth can be formulated using the second vertical derivative values as input anomaly profile as:

$$d_{basement} = \tau S(\Delta g_d(x,y)) \qquad (11)$$

$where\ d_{basement}$= basement depth,

S=shot point spacing,

$\Delta g_{SVD}(x,y) =$ second vertical derivative

τ=constant

Interval velocity determination

By utilizing Figure 2, the interval velocity equation [31] is given as:

$$V_i = 2(\frac{\Delta Z}{\Delta t}) \qquad (11)$$

$V_i =$ interval velocity, $\Delta Z =$ thickness of layer $= Z_{n+1} - Z_n$

$\Delta t =$ vertical two way traveltime through layer $= t_{n+1} - t_n$

Because the interval velocity predicts the travel time through an individual layer, it is the velocity parameter that is included in the seismic model.

The depth normalized interval velocity is expressed [35]:

Citation: Epuh EE, Joshua EO (2017) Basement Depth and Sedimentary Velocity Structure in Gongola Basin. J Geol Geophys 6: 285. doi: 10.4172/2381-8719.1000285

$$V_i^{/} = V_i\left(\frac{Z_n}{Z_m}\right)^{1/N} \qquad (11)$$

$V_i^{/}$ = normalized interval velocity,

V_i = interval velocity,

Z_n = the normalized depth

Z_m = the midpoint depth,

N= compaction value

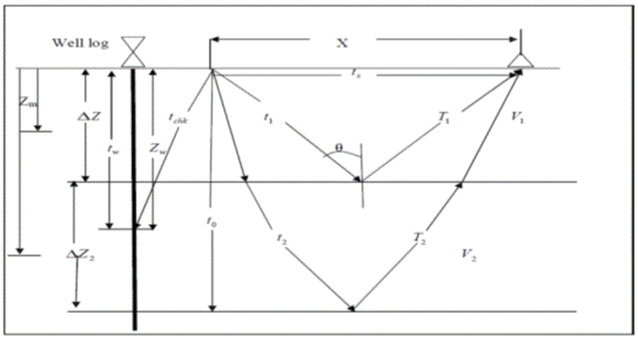

Figure 2: The layered Earth [3].

T_{chk}=Travel time recorded in a check shot offset, t=two way travel time.

T_w=travel time determined from well information, Z_w=depth measured from well information.

q=angle of incidence, X=offset distance, t_o=travel time recorded at zero offset distance.

Methodology

Data acquisition

The gravity data was observed at a total of 1813 gravity stations with station interval of 500 m covering a total distance of 868.45 km. The reflection seismic observation consist 15 crosslines and 8 inlines. The gravity and seismic lines are numbered on the base map as shown in Figure 3.

Data processing

The model of basement depth and deep sedimentary structure that we develop relies on the analysis of gravity, seismic and well log data. The second vertical derivative was computed so as to give a clearer image of the edges of major gravity anomalies and unraveled some subtle trending (lineaments) anomalies that were absent in the Bouguer gravity map.

The computation of the basement using this data gave information on the deeper part of the basin and basement structures. Additionally, the interval and depth normalized interval velocity were used to determine the vertical variation of the strata.

Seven horizons from the seismic sections were tracked for velocity and basement mapping. Since deep sedimentary structure was the primary focus of this investigation, Data from wells drilled were incorporated to determine the formation that of stratigraphic significance in terms of oil and gas investigation.

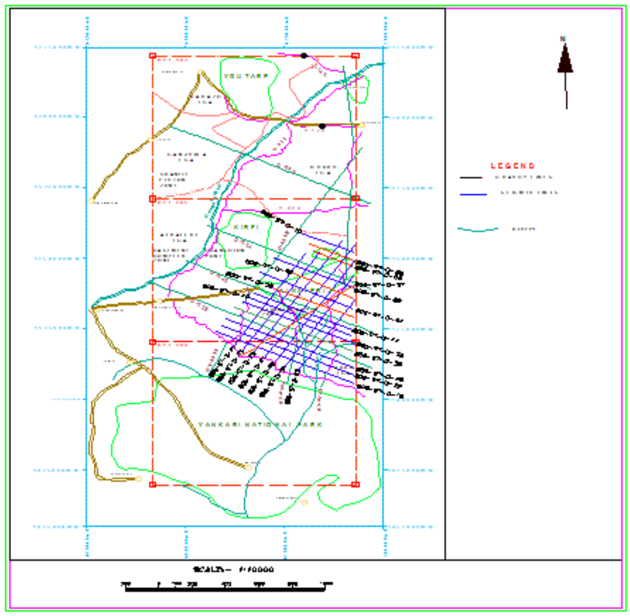

Figure 3: Integrated base map of gravity and seismic lines.

Results and Discussion

The basement depth obtained using the gravity model within the sedimentary basin of the project area has a maximum value of between 5.2 km in the south eastern part and 7.0 km in the north eastern part as shown in Figure 4a. Figure 4b shows the 3-D model of basement showing the ridges along the NE and SE zone of the study area.

The basement depth obtained using the seismic model correlated with that obtained using the gravity model. The basement has listric (concave slope) geometry as obtained from both the gravity and seismic models. The basement obtained using the seismic reflection data is shown in Figure 5a and 5b.

The basement depths obtained from the gravity model were compared with that obtained from reflection seismic observation from the study area (Figure 3) and the relative error percent were 1.37% and 0.46% respectively as shown in Figure 6a and 6b.

Across the Dukku uplift in the far NE of the ma (Figure 4a), basement depth is at least 6.5 km. Along the Northern margin of the Kolmani graben fault system, the basement deepens through faulting into the deepest part of the NE graben system, where basement depth is around 7.0 km.

Although previous investigations are consistent with these general trends in basement depth [13,25], our interpretation generally puts the basement somewhat deeper than the earlier suggestions.

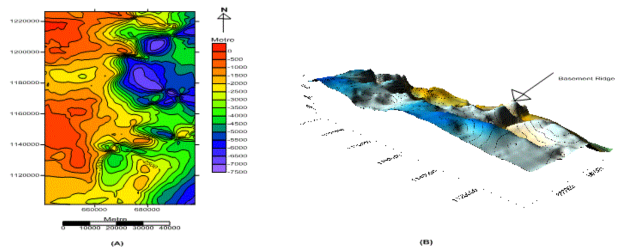

Figure 4: (a) Basement depth map derived from SVD model (C.I=500 m) (b): 3-D model of the basement depth.

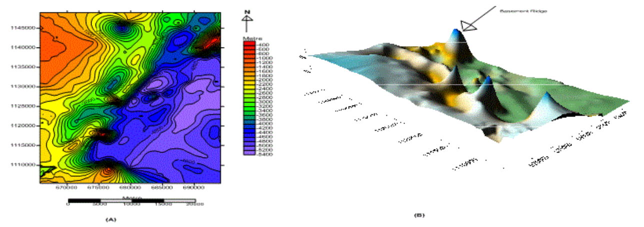

Figure 5: (a): Basement depth obtained from seismic data (b): 3-D model of the basement depth.

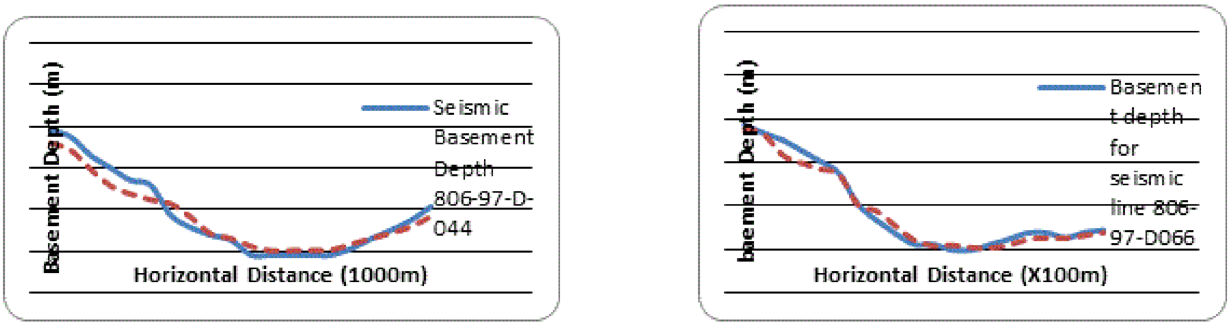

Figure 6 (a,b): Basement depth validation profile for gravity using seismic lines 806-97-D044 and D066.

Velocity model analysis

Figure 7 shows line 806-97-D-36 which depicts the seven horizons, the stratigraphic units and fault geometry which were used for the seismic interpretation. The stack representation of the interval velocity maps are shown in Figure 8. The interval velocities were derived from the seismic reflection results (Figure 7) and the Kolmani well information.

Kerri -kerri (tertiary)

This is the shallowest horizon of all the horizons. The lateral velocity variation is not significant across the entire basin. The resulting lateral velocity variation is due to the effect of geomorphology at the surface. The interval velocity of this horizon varies from 2700 m/s in lead L-A to 2800 m/sin lead L-B, while the depth normalized interval velocity varies from 2810 m/s in lead L-A to 2910 m/s in lead L-B respectively. The lithology identified at this horizon is shale. The uppermost depth normalized interval velocity layer 2.8-2.9 km/s is interpreted as being a superficial covering of weathered and poorly consolidated material underlain by more competent rocks of various ages.

Slight doming of this horizon, as well as the underlying top-of-Cretaceous interface, which was detected and mapped using reflection data and well logs may be due to minor inversion on the north side of the Kolmani graben. Based on the present observed data, no major tertiary deformation has affected the basin hence, the observed flat lying tertiary events which directly lie over a pronounced cretaceous unconformity.

Gombe (upper campanian-maastrichtian)

There was no significant lateral velocity variation at this horizon across the basin. This is due to a unified sediment compaction at this horizon. The interval velocity of this horizon varies from 2700 m/s in lead L-A to 3100 m/s in lead L-B, while the depth normalized interval velocity varies from 2810 m/s in lead L-A to 3220 m/s in lead L-B respectively. The lithology is identified as sandstone and shale [3].

Pindiga (upper cenomanian-campanian)

The lateral velocity variation in this basin has started becoming prominent at this horizon. This is due to differential sedimentation and subsidence. The interval velocity of this horizon varies from 2700 m/s in lead L-A to 3300 m/s in lead L-B, while the depth normalized interval velocity varies from 2810 m/s in lead L-A to 3400 m/s in lead L-B respectively. The horizon shows that the dominant lithology is shale. At these horizons, the lithofacies are uniform. They horizons show similar lithofacies variations because they have the same rate of sedimentation and cementation. The dominant lithology is shale with little presence of sandstone. These horizons fall within the Pindiga stratigraphic formation. The sediment depth is 1600 m (Figure 9a and 9b).

Yolde (cenomanian-turonian)

The lateral velocity variation becomes much more prominent at this horizon displaying its significance between inline 806-97-D-63 and 806-97-D-49 and prograding upward towards the northwest direction. The prominence of the variation is shown in the lead L-B loop closure

Citation: Epuh EE, Joshua EO (2017) Basement Depth and Sedimentary Velocity Structure in Gongola Basin. J Geol Geophys 6: 285. doi: 10.4172/2381-8719.1000285

exhibiting correlation of lithology within the lead. The lead L-A closure is not affected by the prograding of the sediments. The reflection coefficient is 0.01 in L-A and -0.02 in L-B, suggesting that the loop closure in L-B does contain a gas prospect. The interval velocity of this horizon varies from 2750 m/s in lead L-A to 3200 m/s in lead L-B, while the depth normalized interval velocity varies from 2900 m/s in lead L-A to 3330 m/s in lead L-B respectively.

The lithology is identified as gas sand and shale. The variable patterns within the lead L-B lithofacies are as a result of differential sedimentation, cementation and compaction caused by the presence of Gaji and Kolmani Rivers. This also indicates the lateral variation in porosity and permeability of within the lead. The depth structure map of this horizon shows that the lead lies at the depth between 2100 m and 2700 m and this eventually falls within the Yolde/Bima stratigraphic formation. This lead is also recognized at horizons (Bima formation) with depth structural relief of 600 m and 800 m respectively. These horizons fall within the Yolde/Bima stratigraphic formation. Further evaluation of the interval and depth normalized interval velocities shows clearly the presence of gas sand stratigraphic up-dip pinch-outs within the graben.

Between the unconformities (Figure 7), the pattern is one of thickening of sand from northwest to southeast in a downlap fashion. These units thicken in the same direction over a wide region with regard to the local structure. This shows a regional pattern involving landward edge of deposition and progradation with the thickening caused mainly by nourishment because of closeness from the source. The sand sediment is sandstone that has permeability and are of good reservoir quality. This demonstrates that the lead possesses the combination of both structural and stratigraphic trapping potentials [35].

Bima (albian-cenomanian)

At this horizon, the lateral velocity variation becomes more prominent; defining more realistically, the prospect loops closure at L-A and L-B. The variations extend to inline 806-97-D-45. The interval velocity of this horizon varies from 2700 m/s in lead L-A to 4960 m/s in lead L-B, while the depth normalized interval velocity varies from 2910 m/s in lead L-A to 5160 m/s in lead L-B respectively. The lithology is identified as Sandstone (water sand) and shale. It composed predominantly of dolomites and anhydrites, produces good refractions of characteristically high seismic velocity. At this horizon, there is progradation of sandstone towards the northwest part of the project area with the progradation terminating at inline 806-97-D-045. The lithology is identified as dolomite and shale. The horizon lies within the Bima stratigraphic formation. The sediment thickness is 700 m (between the depths of 2700 m and 3400 m respectively).

Bima (lower albian-aptian)

At this horizon, the lateral velocity variation has become erratic extending to the inline 806-97-D- 41. The leads are still defined as in time and depth structure maps extending its area coverage. The interval velocity of this horizon varies from 4450 m/s in lead L-A to 5500 m/s in lead L-B, while the depth normalized interval velocity varies from 4620 m/s in lead L-A to 5800 m/s in lead L-B respectively.. The lithology is identified as Sandstone and shale. At horizon H6, the sandstone progradation has moved up to inline 806-97-D-041. The lithofacies patterns show distinct segmentation caused by variable progradation towards the northwest part of the project area. The sandstone and shale lithological units are segmented because the sediments were distributed and accumulated with changing energy pattern. This horizon lies within the Bima stratigraphic formation.

Precambrian (top basement)

Although no wells penetrate basement rocks in Gongola basin, the basement has not been unambiguously identified on the reflection seismic sections. At this horizon the lateral velocity variation becomes even more erratic. The interval velocity of this horizon varies from 5800 m/s in lead L-A to 6200 m/sin lead L-B, while the depth normalized interval velocity varies from 6100 m/s in lead L-A to 6400 m/s in lead L-B respectively. The lithology is identified as gneiss.

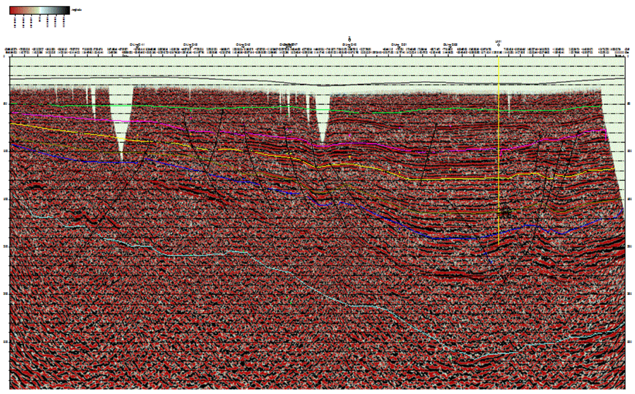

Figure 7: Line 806-97-D-36 showing the stratigraphic units and fault geometry.

Bouguer and derivative map discussion

The results from qualitative interpretation presented in Figure 10 and Figure 11 are based on the analyses of trends and linear contours in the gridded data sets. The map revealed a large-scale negative Bouguer anomaly trending SW-NE and W-E over the central part of the area.

Closer geological and structural observation of this anomaly's axes suggested that its general trend followed an inferred granite intrusion area.

The quite different nature of the Bouguer gravity map on the northern side was marked by gravity lows, bounded by relatively steep gradients occurring over or near higher metamorphic formations and other granitic plutons, suggesting the existence of a suture zone between two of the crustal blocks.

Positive Bouguer gravity in the SW zones shows the dominant presence of basement crystalline rocks, while the positive values in the southern area trending SW-NW marked the intrusion of dense rocks in this area.

The application of the second vertical derivative (Figure 11) involves identifying linear trends on the derivative map that correspond to edges of structures, lithologic contacts and faults [22]. Part of the objective of this work is to unravel subtle linear breaks along the basement using second vertical derivative map.

The prominent anomalies/contour closures are the most geologically significant anomalies on a given map because the help to define the lateral boundary values of the anomalous mass.

Citation: Epuh EE, Joshua EO (2017) Basement Depth and Sedimentary Velocity Structure in Gongola Basin. J Geol Geophys 6: 285. doi: 10.4172/2381-8719.1000285

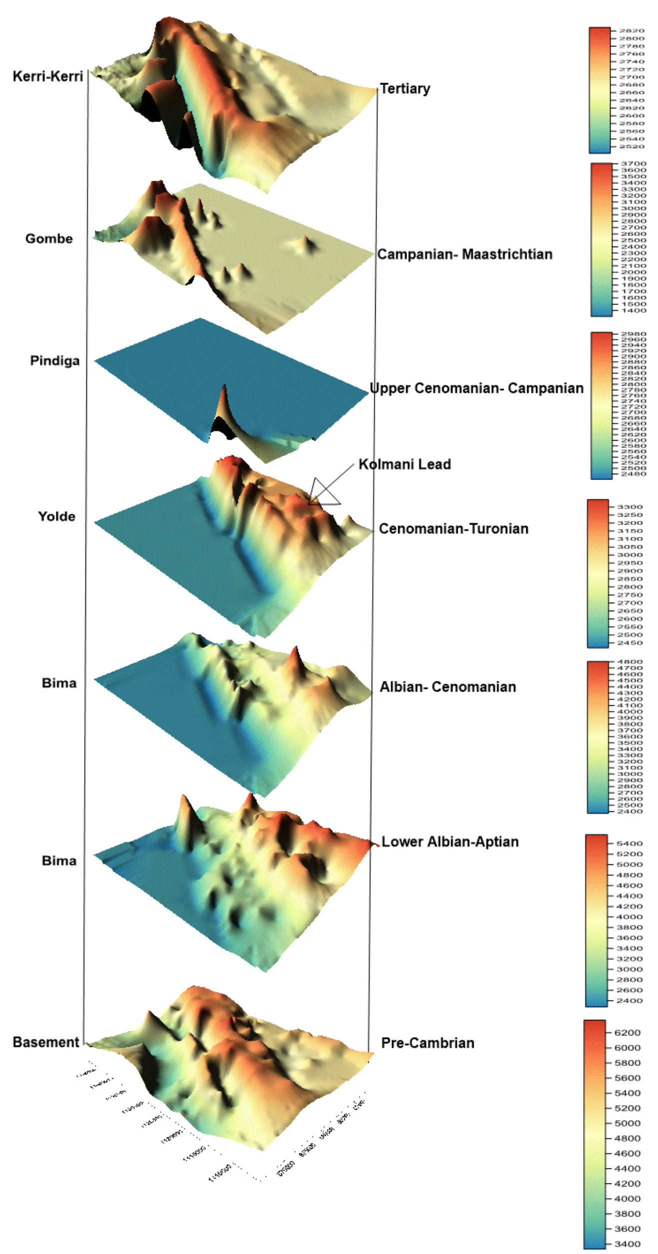

Figure 8: Stack presentation of Horizon Interval Velocity Maps.

The cessation/termination, displacement or interruption of otherwise long or continuous second vertical derivatives anomalies seen in Figure 11 represent significant geologic structural information and are pre-existing weakness in the crust typical of rift zone and deep seated faults that may have been reactivated by stress. The N-S trending lineaments in Figure 11 are interpreted as fault (strike-slip wrench) systems in the upper Benue Trough. Okiwelu et al. [22] opined that the steep gradients evident in the gradient maps are reflection of sharp discontinuities or interfaces between basement blocks of contrasting properties, such as fault, basement shear zones and intrusive contacts.

These are linear features commonly representing lithological contacts, faults, fractures and dyke swarms [36]. The lineaments/faults identified as LF in the gradient map are specifically rift-stage faults associated with vertical rotation (tilting) of fault bounded blocks through which tectonic movement were transmitted. The alignment of these discontinuous, multiple local anomalies in the map represent desirable faults. It shows that the NE-SE zone of the basin series of faults. The anomalies in the gradient maps also show variability in lateral extent and amplitude and are pointers to spatial distribution of half grabens and strike-slip-faulted fabrics.

Structural representation of the basement as shown in the gradient map can therefore serve as an important tool for the prediction of the likely orientation of faults and fractures in the overlying Cretaceous sediments in the trough. These structures within the basement which influence the location of faulting within the sedimentary cover have been reported by Genik, [37] and can also be visualized from the bounded fault blocks (linear contours) in the Northeast and Southeast zones of the basin. Well data by Avbovbo [38] and Epuh et al. [3,35] indicate that the basement rocks underlying Benue Trough are granitic with other acidic rocks such as gneisses and migmatites.

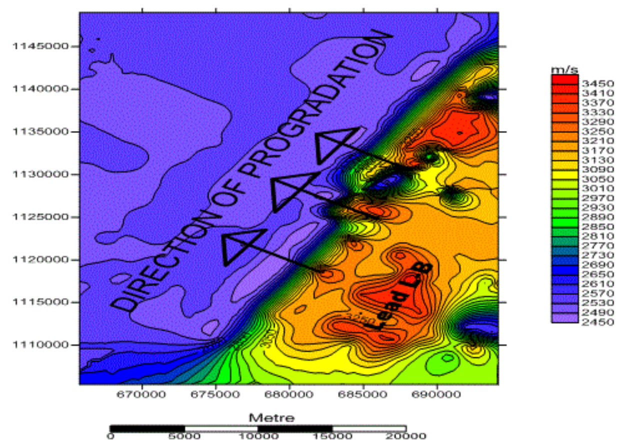

Figure 9a: Yolde (Cenomanian-Turonian) Depth Normalized Interval Velocity Map (contour interval=40 m/s).

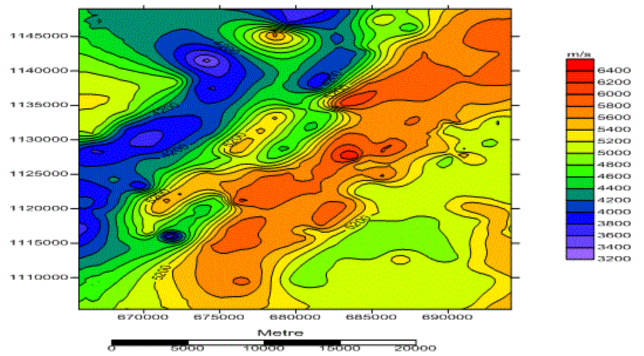

Figure 9b: Top basement (Precambrian) depth normalized interval velocity map (Contour interval=100 m/s).

Citation: Epuh EE, Joshua EO (2017) Basement Depth and Sedimentary Velocity Structure in Gongola Basin. J Geol Geophys 6: 285. doi: 10.4172/2381-8719.1000285

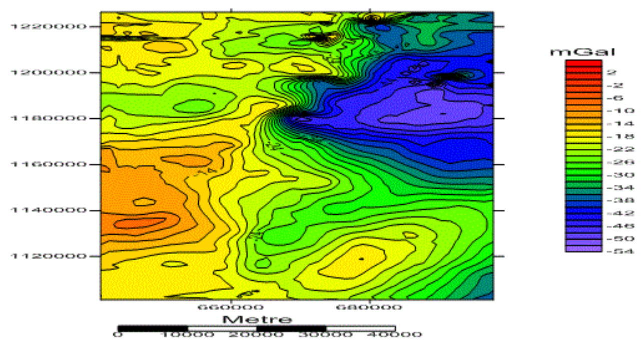

Figure 10: Bouguer anomaly map of the basin.

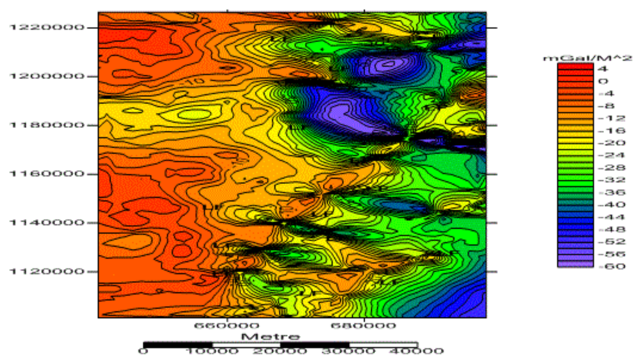

Figure 11: Second vertical derivative map (C.I=2 mGal/m2).

The final basement and velocity model

The basement fracturing, subsidence and rifting visualized from the seismic section (Figure 7) and the transformed/enhanced velocity data and the gravity potential data can be linked to the development of the upper Benue during the Early Cretaceous opening of the South Atlantic Ocean. This active spreading from Albian to Santonian, a period of approximately 30 million years has been established by combined evidence of marine sediments of Albian age, which extend into the Upper reaches of the Benue [39] and the probable limits in igneous/minerlization activity based on sparse radiometric data [40] and geological data [41].

The depth to basement map (Figures 4 and 5) shows series of basement ridges, deep troughs and accommodation zones. The basement arches are important as a means of reconstructing the epirogenic movements that have taken place in the trough [22].

The arches serve as an important requirement for repeated fracture rejuvenation and the fault block rotation that may serve as hydrocarbon plays [22]. The accommodation zones form basement highs and any influx of fluvial sediments can carry clastic material (e.g. sandstone) in the basin to the highs which may serve as hydrocarbon reservoir.

The final velocity model that satisfactorily fits all available data is presented in Figure 12. The velocities in some of the layers change laterally, but layers and in the vertical direction. Well data along the profile, superimposed on the velocity interfaces and their presumed stratigraphic columns. The faulting is steeply dipping (even though the model is oblique to the dominant strike of the area), a result supported by the extensive seismic reflection analysis.

In the area where the reflection transect crosses the Kolmani graben, the velocity model shows that the graben morphology in the upper sedimentary section is similar to the 'classic' model of a normally faulted rift system, more so than elsewhere along the NE/SE of the study area.

Our model shows that this style of faulting persists to basement depth. The model indicates that whilst increasing formation age generally causes increasing seismic velocity, interval velocity is also controlled by depth of burial and, more significantly, by lithology. These, and other ideas, are explored in Figure 9 as each velocity layer, from shallowest to deepest, is discussed in relation to its stratigraphic significance and relevance to regional tectonics. We see a clear trend of deeper basement (7.0 km) to the North East of the basin and shallower basement to the southwest of the Basin (5.2 km).

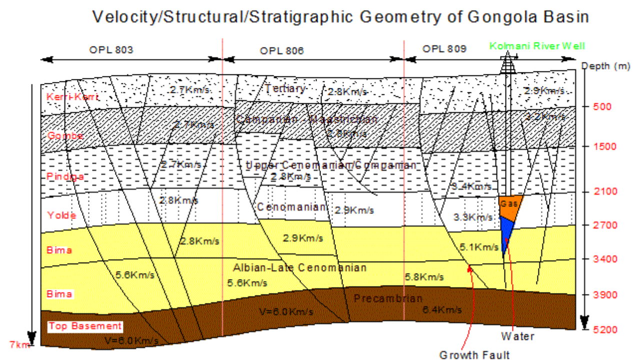

Figure 12: Velocity/structural/stratigraphic geometry of Gongola basin [35].

Conclusion

The depth to basement map (Figure 4b and 5b) shows series of basement ridges, deep troughs and accommodation zones. The mini-basins are interconnected by basement ridges (horsts). The high-angle rift-stage faults and the NE-SE and E-W trending faults controlled the internal geometry of the trough. The basement arches are important as a means of reconstructing the epirogenic movements that have taken place in the trough.

The arches serve as an important requirement for repeated fracture rejuvenation and the fault block rotation that may serve as hydrocarbon plays. The accommodation zones form basement highs and the influx of fluvial sediments carries clastic materials (e.g. sandstone) in the basin to the highs which serve as hydrocarbon reservoir (Figure 12). Basement depth and the location of several deep sedimentary interfaces have been mapped from the interpretation of seismic reflection data, well logs and potential field data.

Hence, extensive thicknesses of pre-Mesozoic rocks and the deeply penetrating faults have been identified in the Gongola graben system, demonstrating the thick-skinned tectonic style of this region. The Incorporation of results from previous research has allowed gross trends in basement depth across Gongola basin as presented in Figure 12. From both geological and geophysical observations, it is suggested that the rifted basins of West and Central Africa are among the best examples of the Mckenzie [42] passive extensional basin model. The Early Cretaceous onset of basin formation in these areas was associated with rifting along the margins of the future South Atlantic [10,22].

Acknowledgments

The data for this study were provided by the Shell Nigeria Exploration and Production Company (SNEPCO).

References

1. Blakely RJ (1996) Potential theory in gravity and magnetics application. Cambridge University Press, United Kingdom.
2. Martinec Z (1993) Effect of lateral density variations of topographical masses in view of improving geoid model accuracy over Canada. Geodetic Survey of Ottawa.
3. Epuh EE, Nwilo PC, Olorode DO, Ezeigbo CU (2012) Application of interval and depth normalized interval velocities in the determination of Gongola Basin Lithology for hydrocarbon exploration. Int J Adv Scien Tech Res 4: 474-490.
4. King LC (1950) Outline and disruption of Gondwanaland. Geol Mag 87: 353-359.
5. Cratchley CR, Jones GP (1965) An interpretation of the geology and gravity anomalies of the Benue Valley, Nigeria. Geophy Papers Overseas Geolog Survey 1: 26.
6. Wright JB (1968) South Atlantic continental drift and the Benue trough. Tectonophy 6: 301-310.
7. Benkhelil J (1982) Benue Trough and Benue chain. Geol Mag 119: 155-168.
8. Whiteman A (1982) Nigeria: it's petroleum geology resources and potential. Graham and Trorman, Londres.
9. Benkhelil J, Robineau B (1983) Is the Benue Trough a rift? Bulletin of Central Research and Exploration Production. Elf- Aquitaine 7: 315-321.
10. Binks RM, Fairhead JD (1992) A plate tectonic setting for Mesozoic rifts of West and Central Africa. Tectonophy 213: 141-151.
11. Coulon C, Vida P, Dupoy C, Baudin P, Pupof M, et al. (1996) The mesozoic to early cenezoic magmatism of the Benue Trough (Nigeria): geochemical evidence for the involvement of the St. Hlena Plume. J Petrol 37: 1341-1358.
12. Abubakar YI, Umegu MN, Ojo SB (2010) Evolution of Gongola Basin upper benue trough Northeastern Nigeria. Asian J Earth Sci 62-72.
13. Shemang Jr EM, Ajayi CO, Umego MN (1998) The structure of the Gongola arm of the upper benue trough as revealed by gravity and magnetic studies. Nigerian Assoc Petrol Explorationist 13: 50-69.
14. Carter JD, Barber W, Tait EA (1963) The geology of parts of Adamawa, Bauchi and Bornu provinces in Northeastern Nigeria. Bulletin Geolog Survey Nigeria 30: 109.
15. Petters SW (1982) Central West African cretaceous-tertiary benthic foraminifera and stratigraphy. Palaeontographica abt 179: 1-104.
16. Petters SW, Ekweozor CM (1982) Petroleum geology of the Benue trough and Southeastern chad basin, Nigeria. AAPG Bulletin 66: 1141-1149.
17. Obaje NG (1994) Coal petrography, microfossils and paleoenvironments of cretaceous coal measures in the middle Bebue Trough of Nigeria. Tuebinger Mikropalaeontologishe 11: 1-165.
18. Obaje NG, Attah DO, Opeloye SA, Moumouni A (2006) Geochemical evaluation of the hydrocarbon prospects of sedimentary basins in northern Nigeria. Geochemical J 40: 227-243.
19. Avbovbo AA, Ayoola EO, Osahon GA (1986) Depositional and structural styles in the chad basin of northeastern Nigeria. AAPG Bulletin 70: 1787-1789.
20. Olugbemiro RO, Ligouis B, Abaa SI (1997) The cretaceous series in the chad basin, NE Nigeria: source rock potential and thermal maturity. J Petrol Geol 20: 51-58.
21. Ofoegbu CO, Onuoha KM (1990) Analysis of magnetic data over the Abakiliki Anticlinorium of the lower Benue Trough, Nigeria. Mar Petrol Geol 8: 174-183.
22. Okiwelu AA, Okwueze EE, Akpan PO, Ude IA (2015) Basin framework and basement structuring of lower Benue Trough, West Africa based on regional magnetic field data: Tectonic and Hydrocarbon Implications. Earth Science Research 4.
23. Adighije CI (1981) Gravity study of lower Benue Trough, Nigeria. Geol Mag 118: 59-67.
24. Ajayi CO, Ajakaiye DE (1981) The origin and peculiarities of the Nigerian Benue Trough-another look from recent gravity data obtained from the Middle Benue. Tectonophy 80: 285-303.
25. Okereke CS, Ofoegbu CO, Ezeanyim VI (1990) Cretaceous sediment thickness in the Benue Tough, Nigeria, determined from gravity interpretation. Bullett. DI Geofisica Teorica ED Appl 128: 257-266.
26. Fairhead JD (2012) Regional tectonics and basin formation: The role of potential field studies in Phanerozoic. Regional Geol world 12: 330-341.
27. Oyedim GC, Alagoa KD, Adedokun IO, Aderogb AA, Ovuru CC (2009) Mapping high-angle basement faults in the middle Benue Trough, Nigeria from gravity inversion surface. Earth Sci Res J 13: 140-147.
28. Burke KC, Dessauvagie TFJ, Whiteman AJ (1970) Geological history of the Benue Valley and adjacent areas. University of Ibadan, Ibadan.
29. Fitton JG (1980) The Benue Trough and Cameroon line-a migrating rift system in West Africa. Earth Planet Sci Letters 51: 132-138.
30. Petters SW (1978) Stratigraphic evolution of the Benue Trough and its implications for the upper cretaceous paleogeography of West Africa. J Geol 86: 311-322.
31. Dobrin MB, Savit CH (1988) Introduction to Geophysical Prospecting (4th Edn) McGrawHill Book Co. Singapore.
32. Bullard EC, Cooper RI (1948) Determination of the masses required to produce a given gravitational field. Royal Soc Proc 194: 332-347.
33. Grant FS, West GF (1987) Interpretation Theory in Applied Geophysics. McGrawhill Book Company, Toronto.
34. Epuh EE, Nwilo PC, Olorode DO, Ezeigbo CU (2011) Basement depth estimation of the Gongola Basin using second vertical derivative data as input anomaly profile. Eur J Scien Res 61: 174-183.
35. Epuh EE, Nwilo PC, Olorode DO, Ezeigbo CU (2012) Petrophysical characterization of Gongola Basin (Kolmani River -1) shaly-sand reservoir using dual water model. J Asian Scien Res 2: 170-181.
36. Olaniyan O, Smith RS, Morris B (2013) Qualitative geophysical interpretation of the sudbury structure. Interpretation 1: 25-43.
37. Genik GJ (1992) Regional framework and structural aspects of rift basins in Niger, Chad and the Central African Republic (C.A.R.) Tectonophy 213: 169-185.
38. Avbovbo AA (1980) Basement geology in the sedimentary basins of Nigeria. Geology 8: 323-327.
39. Grant NK (1971) South Atlantic, Benue Trough and Gulf of Guinea Cretaceous tripple junction. Geol Society of American Bulletin 82: 2395-2298.
40. Snelling NJ (1965) Age determination unit, in Annual Report Institute Geological Sciences for 1964.
41. Offodile ME (1976) The Geology of the Middle Benue, Nigeria. Palaentological Institute, University of Uppsala, Special Publication 4: 1-166.
42. Mckenzie DP (1978) Some remarks on the development of sedimentary basins. Earth Planet Scienc Letters 40: 25-32.